Receiver Cancellation of Radar in Radio†

Kathleen L. Tokuda#, Joseph H. Kim*, Robert J. Baxley*#, J. Stevenson Kenney#, and Lawrence S. Cohen+

#Georgia Institute of Technology, Atlanta, GA 30332, USA
*Georgia Tech Research Institute, Atlanta, GA 30318, USA
+Naval Research Laboratory, Washington, DC 20375, USA

***Abstract*— Global pressure to use spectrum more efficiently has sparked a great deal of research to mitigate spectral and spatial congestion between radar and radio systems operating in a shared spectrum access environment. This paper summarizes an algorithmic method of interference cancellation that enables the radar and radio to operate with reduced spatial and spectral separation. These performance improvements are achieved by modeling the measured spectral broadening due to nonlinear effects at the radar transmitter and cancelling this out-of-band interference at the communications receiver. Subsampling to address hardware constraints on receiver bandwidth and to achieve data (complexity) reduction is shown to be feasible.**

I. Introduction

Interference cancellation is a promising approach to improve performance and enhance spectral efficiency in shared spectrum access for radar and communications (SSPARC) systems. Such techniques are based on accurate models of a power amplifier (PA) and/or side information about a radar transmission to enable a communications receiver to estimate and cancel adjacent-band spectral leakage from a radar transmitter [1]. Given a specific PA model, we can represent the transmitted signal $\boldsymbol{y}$, a column vector of N collected samples, as

$$\boldsymbol{y} = \boldsymbol{A}\boldsymbol{c}, \tag{1}$$

where $\boldsymbol{A}$ is an N x κ matrix representing the system equations of a PA model in terms of an input signal $\boldsymbol{x}$, and $\boldsymbol{c}$ is a κ x 1 vector of model coefficients. The objective of PA modeling is to find $\boldsymbol{c}$ in (1), characterizing the nonlinearities of the amplifier. While this system is nonlinear in inputs $\boldsymbol{x}$, it can be linear in system coefficients $\boldsymbol{c}$; hence, a least-squares solution may be obtained by computing the pseudoinverse of $\boldsymbol{A}$, as in

$$\boldsymbol{c} = \boldsymbol{A}^{-1}\boldsymbol{y}. \tag{2}$$

Recent trends in PA modeling [2]–[5] favor variations of a Volterra model

$$y(t) = \sum_{k=1}^{K} \int \dots \int h_k(\boldsymbol{\tau}_k) \prod_{i=1}^{k} x(t-\tau_i) d\boldsymbol{\tau}_k \tag{3}$$

where $y(t)$ and $x(t)$ are the output and input of a PA, respectively, K is maximum nonlinear order, t is time, and τ_i represents delay. The terms $h_k(\boldsymbol{\tau}_k)$ are the Volterra coefficients [2] populating $\boldsymbol{c}$ in (1) and (2). The main disadvantage of the Volterra model is that it often requires a large number of coefficients. Also, the accuracy of this approach may be degraded if the system of coefficient equations is ill-conditioned, leading to significant changes in output results for relatively small fluctuations in the input data. "Pruning," or using a subset of the model [3], and special cases, *e.g.*, memory polynomials representing the diagonal terms of the Volterra model [4], have been considered to reduce computational complexity, but these methods still have accuracy issues if ill-conditioned. In [5], this issue is addressed by creating orthogonal polynomial basis functions in the signal sample space, leading to better convergence and improved numerical stability.

In the remainder of this paper, we compare the results of using a Volterra versus an orthogonal memory polynomial (OMP) model to estimate and cancel radar spectral distortion interference to a communications receiver to improve spectral efficiency in SSPARC systems.

II. Measurements and Post-Processing

A. Measurements

Fig. 1 is a block diagram of the measurement testbed with a photo of the actual setup. The testbed consists of a National Instruments PXIe-8130 embedded controller, two PXIe-5663 6.6-GHz RF vector signal analyzers (RFSAs) with 50-MHz instantaneous bandwidth, a PXIe-5673 6.6-GHz RF vector signal generator (RFSG) with 100-MHz instantaneous bandwidth, and an HP E4433B signal generator (ESG). Measurements are automated in NI LabVIEW. Using this setup, a wideband radar interference signal generated with the RFSG is fed to a PA, then summed with a signal from the ESG representing a narrowband desired communications signal. Both are implemented as band-limited additive white Gaussian noise (AWGN), a scenario typically considered to be worst case. The PA input and output (radar-only reference), and test signal (communications plus radar waveform) are measured for post-processing.

†The views expressed are those of the authors and do not reflect the official policy or position of the Department of Defense or the U.S. Government. Approved for Public Release, Distribution Unlimited.

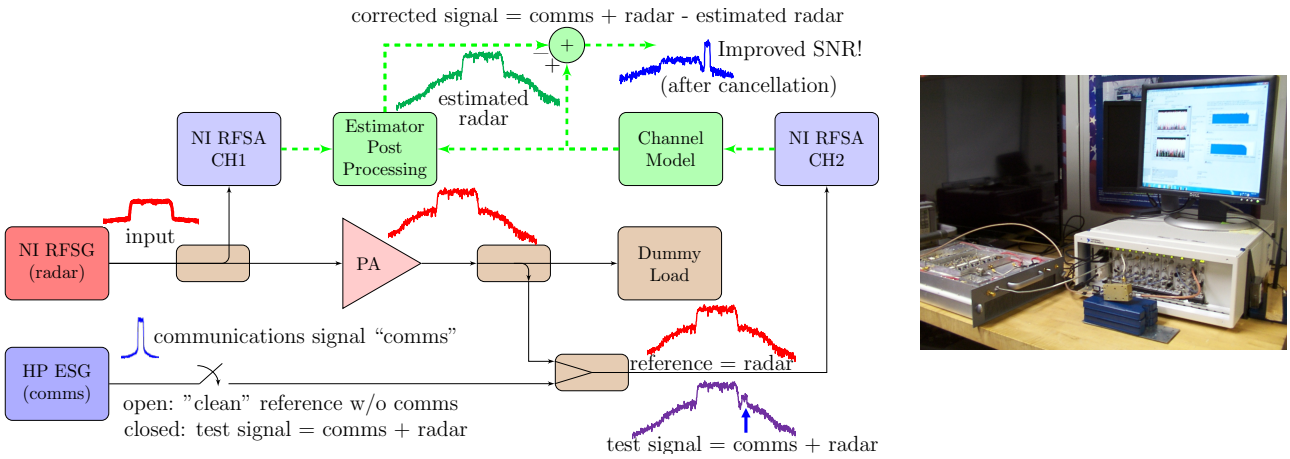

Fig. 1. Block diagram and photo of measurement setup.

B. Post-Processing of Measured Data

The measured data is post-processed in MATLAB to obtain coefficients $\boldsymbol{c}$ using (2) for a Volterra model [2] with order $K = 5$ and memory length $M = 4$ and an OMP model [5] with $K = 12$ and $M = 7$, where M represents a delay, or memory length, *i.e.*, the longest delay is represented by $M - 1$ sampling steps. For either case, the extracted model is used to generate an estimate of the adjacent-band spectral expansion

$$\hat{\boldsymbol{y}} = \boldsymbol{A}\boldsymbol{c}, \tag{4}$$

using $\boldsymbol{c}$ from (2) given measured data for $\boldsymbol{y}$, and sufficient side information to construct $\boldsymbol{A}$. This estimated cancellation signal $\hat{\boldsymbol{y}}$ is subtracted from the received test signal in MATLAB to improve received signal-to-interference-plus-noise ratio (SINR).

C. Practical Considerations: Subsampling

Typical communications receivers have relatively small bandwidths compared to that of a radar waveform. Unless receiver hardware modifications are made, only a fraction or "subband" of the full radar bandwidth is observed by the receiver, and the radar out-of-band interference must be estimated without sampling the full radar bandwidth. To demonstrate feasibility of the cancellation approach based on subband sampling or subsampling the radar signal, the output radar waveform from the PA is shifted in frequency by 5 MHz, low-pass filtered to 2.4 MHz, and downsampled to emulate subsampling by a communications receiver. Since the communications signal's carrier frequency is offset from the radar's center frequency, the input radar waveform is shifted to align in frequency with the communications signal. The model matrix $\boldsymbol{A}$ is generated from this shifted input radar waveform, then the matrix is downsampled to match the communications signal's sampling rate, including an anti-aliasing filter matching the bandwidth of the communications signal. The downsampled model matrix and the subsampled communications signal are used to calculate the model coefficients using (2) and to generate a cancellation signal as in (4). Since the model matrix $\boldsymbol{A}$ is downsampled, and therefore reduced in size, the computational time and complexity is also reduced.

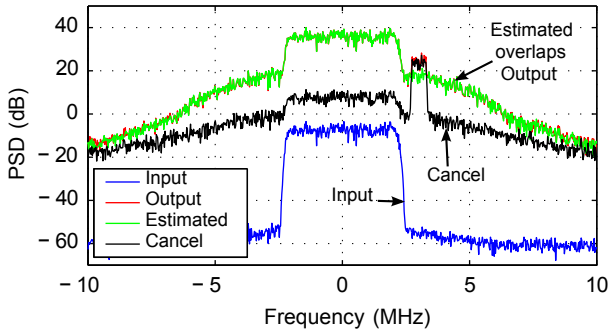

Fig. 2. Measured PSDs for the input and test output (interference plus desired signal) with post-processed traces for a P_{in} of 12 dBm. Note that the output and estimated traces overlap.

III. Results

Referring to the measurement set-up of Fig. 1, the input, reference, and test signals are measured. Fig. 2 shows the corresponding power spectral density (PSD) for each signal, given an input power of 12 dBm. The model-based estimate of the interference is also shown, overlapping the output, with the improved signal after cancellation, *i.e.*, after subtracting the estimate from the combined test signal output. The SINR may be estimated from an average of the desired signal level and an average of the signal level adjacent to the desired signal. For example, the SINR of the desired signal before post-processing of the output signal is ∼4 dB. After interference cancellation, the SINR of the desired signal is ∼22 dB, representing ∼18 dB of interference suppression. The device under test, for the dataset represented in Figs. 2–5 is a high-power Class AB PA optimized for a center frequency of 2.14 GHz.

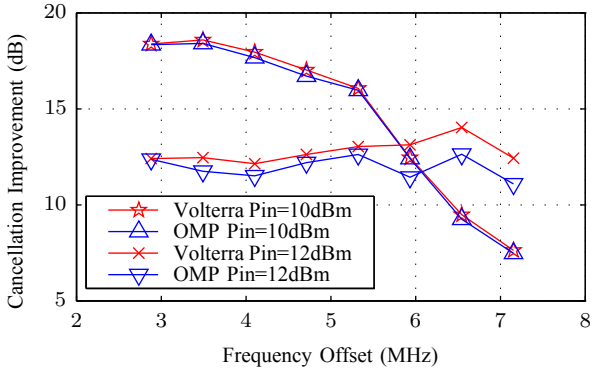

Fig. 3. Cancellation improvements versus frequency offset for an orthogonal memory polynomial ($M = 7$, $K = 12$) and a Volterra model ($M = 4$, $K = 5$) for input powers of 10 and 12 dBm.

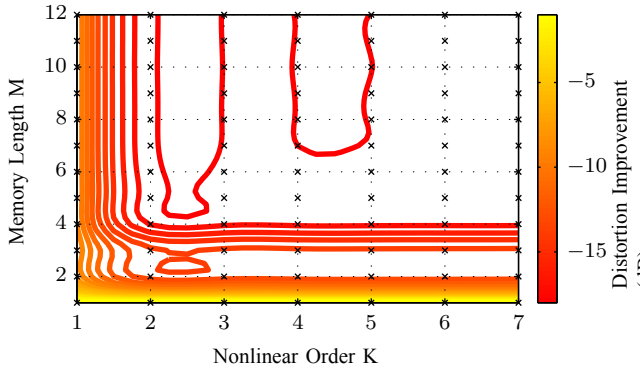

Fig. 4. Distortion improvement contours for an orthogonal memory polynomial, frequency offset ∼3.5 MHz, P_{in} is 12 dBm.

Fig. 3 compares the performance of an OMP and a Volterra model in a plot showing interference suppression, over a frequency offset range of 2.5–7.5 MHz, where each plotted point represents an average over a 0.5-MHz bandwidth. These models track each other for the different power levels shown. Increasing the input power level causes more distortion and this increase in distortion leads to an increase in cancellation improvement. Although the Volterra model achieves similar performance with lower order and memory length, it requires 1364 coefficients while the OMP model only requires 84 coefficients, resulting in a significant decrease in computational load.

Fig. 4 is a contour plot showing distortion improvement as a function of model order and memory length for an OMP corresponding to a 3.5-MHz offset. This figure illustrates that increased modeling does not necessarily lead to better results, indicated by regions where increasing order or memory length does not improve performance.

In Fig. 5, SINR before and after interference cancellation is shown as a function of distance using a simple path-loss model, and as a function of varying amounts of AWGN at the receiver, *i.e.*, versus receiver signal-to-noise ratio (SNR). By inspection of Fig. 5(a),

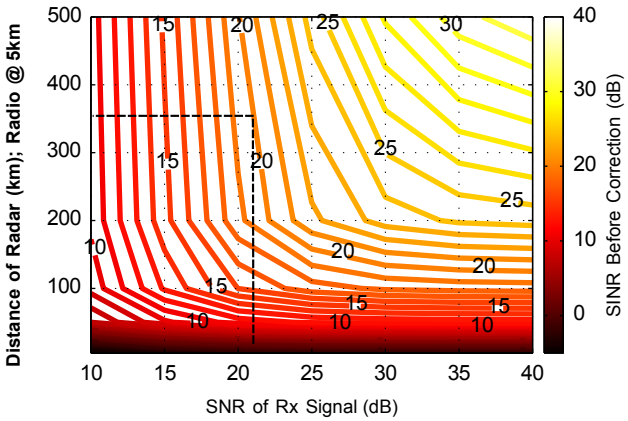

(a) Before interference cancellation.

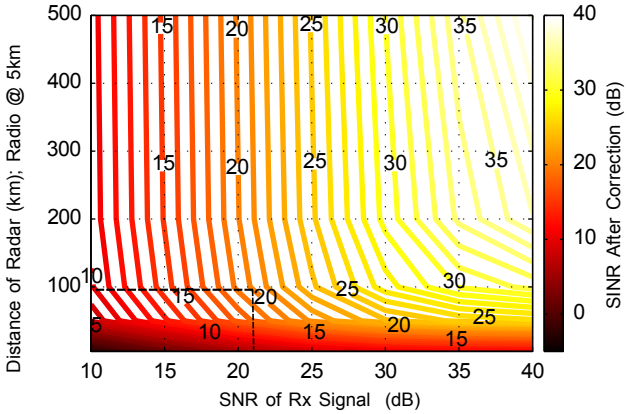

(b) After interference cancellation.

Fig. 5. SINR for varying SNR of received signal and distance of radar before and after interference cancellation.

before distortion correction, given a receiver SNR of ∼21 dB, a receiver target SINR of 20 dB can be achieved when the radar is 300 km away from the receiver. From Fig. 5(b), after distortion correction, the radar can be as near as ∼100 km, and maintain the same target SINR of 20 dB and SNR of ∼21 dB, indicating that the radar–radio separation can be reduced when using interference cancellation.

Fig. 6 shows the results of subsampling an Amplifier Solutions Corporation (ASC2082C) phased-array radar PA operating at 3 GHz. In post-processing, we assume a 5-MHz radio bandwidth (dashed rectangle) centered 2.5 MHz beyond the band edge of the radar. This example shows SINR improvement of ∼20 dB is achieved with subsampled estimation and cancellation, indicating that nonlinear out-of-band distortion from the radar can be effectively estimated and cancelled, without sampling the full bandwidth of the radar.

IV. Conclusion

Measured and post-processed data indicate performance improvements due to cancellation of radar interference by

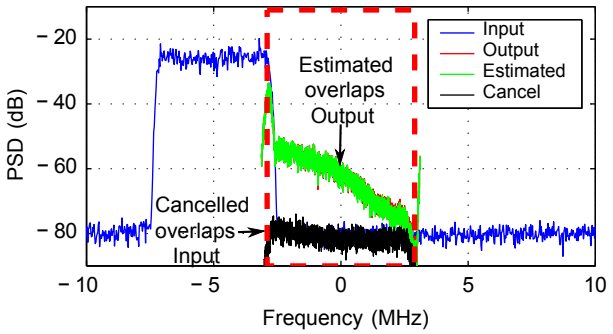

Fig. 6. PSDs for subsampled communication signal with full radar input waveform. The dashed rectangle indicates the subsampled radar output bandwidth. Note that the output and estimated traces overlap.

a communications receiver of up to ∼20 dB of receiver-side distortion mitigation, which corresponds to a significant reduction in radar-communications separation. These results indicate that radar interference cancellation by a communications receiver is a promising topic for further research relevant to SSPARC.

ACKNOWLEDGMENT

This project is sponsored by the Defense Advanced Research Projects Agency, Strategic Technology Office Program: SSPARC.

REFERENCES

[1] E. L. Mokoke and L. S. Cohen, "A summary of spectrum engineering, the why and how," in *2013 U.S. Nat. Committee URSI Nat. Radio Science Meeting*, Jan. 2013, p. 1.

[2] A. Zhu, J. Dooley, and T. Brazil, "Simplified Volterra series based behavioral modeling of RF power amplifiers using deviation-reduction," in *IEEE MTT-S Int. Microwave Symp. Dig.*, June 2006, pp. 1113–1116.

[3] A. Zhu, J. Pedro, and T. R. Cunha, "Pruning the Volterra series for behavioral modeling of power amplifiers using physical knowledge," *IEEE Trans. Microwave Theory and Tech.*, vol. 55, no. 5, pp. 813–821, May 2007.

[4] L. Ding, G. Zhou, D. Morgan, Z. Ma, J. Kenney, J. Kim, and C. Giardina, "A robust digital baseband predistorter constructed using memory polynomials," *IEEE Trans. Communications*, vol. 52, no. 1, pp. 159–165, Jan. 2004.

[5] R. Raich, H. Qian, and G. Zhou, "Orthogonal polynomials for power amplifier modeling and predistorter design," *IEEE Trans. Vehicular Technology*, vol. 53, no. 5, pp. 1468–1479, Sept. 2004.